



The neuronal nitric oxide synthase expression increases during satellite cell-derived primary myoblasts differentiation

Masaki Kusano^{1,2}, Kazuya Sakai¹, Yuki Tomiga^{1,3}, Ai Ito¹, Shihoko Nakashima⁴, Yoshinari Uehara^{1,4},
Kentaro Kawanaka^{1,4}, Yasuo Kitajima⁵, Yasuki Higaki^{1,4*}

¹The Fukuoka University Institute for Physical Activity, Fukuoka University, 8-19-1 Nanakuma, Jonan-ku, Fukuoka 814-0180, Japan

²Graduate School of Sports and Health Science, Fukuoka University, 8-19-1 Nanakuma, Jonan-ku, Fukuoka 814-0180, Japan

³Division of Metabolism and Endocrinology, Faculty of Medicine, Saga University, 5-1-1 Nabeshima, Saga 849-8501, Japan

⁴Faculty of Sports and Health Science, Fukuoka University, 8-19-1 Nanakuma, Jonan-ku, Fukuoka 814-0180, Japan

⁵Department of Immunology, Graduate School of Biomedical and Health Sciences, Hiroshima University, 1-2-3 Kasumi, Minami-ku, Hiroshima 734-8551, Japan

ARTICLE INFO

Original paper

Article history:

Received: May 30, 2023

Accepted: September 17, 2023

Published: December 10, 2023

Keywords:

Primary myoblast, muscle satellite cells, neuronal nitric oxide synthase, DNA methylation, muscle differentiation

ABSTRACT

The neuronal nitric oxide synthase (nNOS; encoded by *NOS1*)-derived nitric oxide (NO) plays an important role in maintaining skeletal muscle mass. In adult skeletal muscle, nNOS localizes to the cell membrane, cytosol, and nucleus, and regulates muscle hypertrophy and atrophy in various subcellular fractions. However, its role in muscle stem cells (also known as muscle satellite cells), which provide myonuclei for postnatal muscle growth, maintenance, and regeneration, remains unclear. The present study aimed to determine nNOS expression in muscle satellite cell-derived primary myoblasts during differentiation and its DNA methylation levels, an epigenetic modification that controls gene expression. Undifferentiated and differentiated satellite cell-derived primary myoblasts were found to express nNOS. Immunohistochemical analysis revealed that nNOS colocalized with Pax7 (satellite cell marker) only in the undifferentiated myoblasts. Furthermore, nNOS immunoreactivity spread to the cytosol of Pax7-negative differentiated myotube-like cells. The level of *Nos1 μ* mRNA, the main isoform of skeletal muscle nNOS, was increased in differentiated satellite cell-derived primary myoblasts compared to that in the undifferentiated cells. However, *Nos1* methylation levels remained unchanged during differentiation. These findings suggest that nNOS induction and the appropriate transition of its subcellular localization may contribute to muscle differentiation.

Doi: <http://dx.doi.org/10.14715/cmb/2023.69.13.20>

Copyright: © 2023 by the C.M.B. Association. All rights reserved.

Introduction

Maintaining skeletal muscle mass is essential for a healthy and active life. Epidemiological evidence suggests that skeletal muscle mass and strength are associated with all-cause mortality (1, 2). The myofiber is the cellular unit of the adult skeletal muscle, and its repair and maintenance are assigned to muscle satellite cells located beneath the basal lamina (3). Activation and proliferation of satellite cells are important events in the repair and regeneration of damaged muscles (4).

Nitric oxide (NO), a well-known air pollutant, is a known regulator of skeletal muscle mass. NO is synthesized from its precursor L-arginine by three isoforms of NO synthase (NOS): neuronal NOS (Nnos), inducible NOS (Inos), and endothelial NOS (Enos). Nnos is located in the skeletal muscle cell membrane (5) and is involved in muscle hypertrophy and atrophy. Unloading, such as cast immobilization or hindlimb suspension, decreases nNOS protein levels (6), resulting in the translocation of Nnos from the cell membrane to the cytosol and subsequent production of NO, which initiates muscle atrophy (7). However, eNOS, another constitutive isoform of NOS in skeletal muscles, does not affect disuse-induced muscle atrophy (7). Meanwhile, nNOS activation via synergistic

ablation regulates overload-induced muscle hypertrophy (8). Thus, nNOS-derived NO plays a role in regulating skeletal muscle mass.

nNOS-derived NO regulates muscle regeneration by regulating satellite cells. The number of satellite cells increases after treatment with NO donors, whereas that in nNOS-depleted animals is significantly decreased (9). In addition, the regenerating muscles in nNOS knockout mice show a smaller myofiber cross-sectional area (10) and the recovery from cardiotoxin-induced muscle damage is delayed (9) than that in wild-type mice. These findings highlight the importance of the effects of nNOS-derived NO on skeletal muscle and satellite cells. However, the role and endogenous expression levels of nNOS in satellite cells during the differentiation process remain unclear.

Muscle satellite cell differentiation is regulated by DNA methylation, a major epigenetic modification, carried out by DNA methyltransferase (DNMT) 3a (11). Previously, we reported that cast immobilization-induced unloading decreased nNOS mRNA expression and increased DNA methylation levels (6). This finding suggests that nNOS DNA methylation may be a target for muscle mass regulatory mechanisms; however, this study only analyzed whole muscle tissues, such as the soleus and extensor digitorum longus. Therefore, the expression and regulatory mecha-

* Corresponding author. Email: higaki@fukuoka-u.ac.jp

nisms of nNOS in satellite cells, which form the basis of muscle mass regulation, remain unclear.

This study aimed to determine whether nNOS expression in skeletal muscle satellite cell-derived myoblasts changes during differentiation and whether DNA methylation is involved in this change.

Materials and Methods

Animals

Male C57BL/6J mice (n = 16, 9 weeks old; CLEA Japan Inc., Tokyo, Japan) were used in this study. The animals were housed in an accredited animal facility room under a 12:12 h light/dark cycle. Animals were fed standard chow and water ad libitum. All the experiments were approved by the Animal Care and Use Committee of Fukuoka University (approval number: 1911093).

Satellite cell-derived primary myoblast isolation and culture

Satellite cells were isolated from the gastrocnemius muscle by the pre-plating method according to our previous report (12). Although this method can provide high yield and purity of muscle stem cells, these cells include activated and quiescent satellite cells. Therefore, we defined these cells as “satellite cell-derived primary myoblasts” in this study. The experimental procedure used in this study is illustrated in Figure 1. First, the gastrocnemius muscle was isolated from both legs of mice after cervical dislocation and placed in Dulbecco’s phosphate-buffered saline (D-PBS; Wako, Osaka, Japan). To obtain a sufficient number of primary myoblasts, the gastrocnemius muscles of two mice were used as one sample. Muscle tissues were minced three hundred times, then placed into Dulbecco’s modified Eagle’s medium (DMEM; Thermo Fisher Scientific, MA, USA) containing 0.2% collagenase Type II (Worthington Biochemical, NJ, USA) and 1% penicillin-streptomycin (Wako, Osaka, Japan), and incubated at 37°C for 60 min. Tissue lysates were suspended using an 18G needle and then re-incubated at 37°C for 30 min. After resuspension, D-PBS was added to tissue lysates until the volume reached 30 ml. After straining the tissue lysates, primary myoblast cells were separated from the supernatant by centrifugation (1500 rpm for 5 min at 4°C). Thereafter 30 ml of PBS containing 2% FBS (Thermo Fisher Scientific) was added to the cell pellet, followed by centrifugation (1500 rpm for 5 min at 4°C). Then, 4 ml of growth medium (GM; DMEM, 30% FBS, 1% Chick Embryo Extract (USBiological, MA, USA), 5 ng/ml basic fibroblast growth factor (Oriental Yeast Co., Ltd., Tokyo, Japan) was added to the cell pellet, followed by centrifugation and resuspension of the cell pellet in a 60 mm collagen-coated dish (AGC Techno Glass Co., Shizuoka, Japan). The primary myoblast cells were cultured at 37°C in a humidified atmosphere with 5% CO₂ for 15 h. The dish was gently shaken to suspend unattached cells, which were then displaced to different dishes. After 3 h, primary myoblasts were seeded on Matrigel matrix basement membrane (Corning, NY, USA)-coated 6-well plates, and the GM was changed after 48 h. Cells harvested from the GM on day 4 were designated as the d4 primary myoblast (d4PM) cells, and these comprised undifferentiated primary myoblasts. The medium was changed from GM to differentiation medium (DM; DMEM containing 2% horse

serum) on day 5. Cells harvested from the DM on day 6 were designated as d6 primary myoblast (d6PM) cells, and these comprised differentiated primary myoblasts (Figure 1).

Immunohistochemistry

Immunohistochemistry of primary myoblasts was performed as described in our previous study (13). Briefly, d4PM and d6PM cells were fixed with 4% paraformaldehyde (Wako, Osaka, Japan) at room temperature for 10 min. The cells were washed five times for 3 min each in PBS containing 0.025% Tween 20. The cells were then incubated with blocking buffer (PBS with 0.3% Triton X-100 containing 5% goat serum) for 20 min and washed five times. The samples were then incubated with the following primary antibodies overnight at 4°C: anti-paired box transcription factor 7 (Pax7; Chicken/Human/Mouse/Rat, Mouse-Mono [MAB1675]; dilution 1:400), and rabbit polyclonal anti-nNOS (61-7000; dilution 1:100). The cells were then washed five times, and incubated with the following secondary antibodies for 60 min at room temperature: Alexa Fluor® 488 Goat Anti-Mouse IgG H&L (A-11001; dilution 1:1000) and Alexa Fluor® 594 Goat Anti-Rabbit IgG H&L (A-11012; dilution 1:1000). After washing five times, the nuclei counterstained with DAPI (VECTOR LABORATORIES Inc, California, USA). Subsequently, cells were observed under a fluorescence microscope (FSX100; Olympus, Tokyo, Japan).

Western blot analysis

Total protein was extracted from d4PM and d6PM cells as described previously 6. Samples (8 µg total protein per lane) were separated on a 4–15% precast polyacrylamide gel (Bio-Rad) and transferred onto a polyvinylidene fluoride membrane (Millipore, MA, USA) using semi-dry methods. After transfer, the membrane was blocked with 3% skim milk at room temperature for 1 h. Then, the membrane was incubated overnight at 4°C with the following primary antibodies: primary rabbit polyclonal anti-nNOS (#N-7280, Sigma-Aldrich, Buchs, Switzerland) and anti-GAPDH (#ACR001 P, Acris Antibodies, Herford, Germany). The membranes were then incubated with horseradish peroxidase-conjugated anti-mouse IgG antibody (PI-2000; Vector Laboratories, Burlingame, CA, USA) for 1 h at room temperature. Bound antibodies were detected using ECL Select Western Blotting Detection Reagent (Amersham Bioscience, Piscataway, NJ, USA) and analyzed using an Amersham Imager 600 (GE Healthcare Life Science, Tokyo, Japan). Band densities were determined using Image Lab software (Bio-Rad). The nNOS protein levels were normalized to GAPDH protein levels.

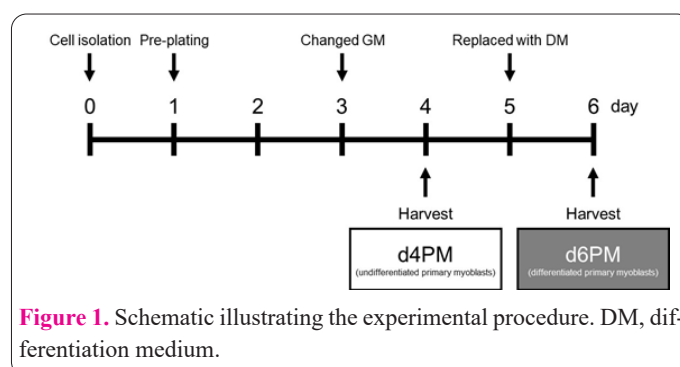


Figure 1. Schematic illustrating the experimental procedure. DM, differentiation medium.

Gene expression analysis

Total RNA was extracted using a Fast Gene RNA Basic Kit ((FG-80050, Nippon Genetics Co., Ltd, Tokyo, Japan), and its concentration and purity were measured using NanoDrop 2000 (Thermo Fisher Scientific). Isolated RNA (200 ng) was reverse-transcribed to cDNA using Primer-Script RT Master Mix (Takara Bio, Shiga, Japan). Quantitative real-time polymerase chain reaction (qRT-PCR) was performed using THUNDERBIRD® Next SYBR® qPCR Mix, (QPX-201, Toyobo CO., LTD, Osaka). The primers used were: *Nos1* exon 1a and 2 specific (*Nos1 μ*) forward and reverse primers (forward: 5'-GCT CGG CAG CAG CTC CAG GTA-3' and reverse: 5'-TCA AGG TTG ACC AGG CAG ACG-3'), *Pax7* forward and reverse primers (forward: 5'-GTG CCC TCA GTG AGT TCG ATT AGC-3', reverse: 5'-CCA CAT CTG AGC CCT CAT CCA-3'), myogenic differentiation 1 (*MyoD*) forward and reverse primers (forward: 5'-CTA CAG GCC TTG CTC AGC TC-3', reverse: 5'-AGA TTG TGG GCG TCT GTA GG-3'), *Myogenin* forward and reverse primers (forward: 5'-CTA CAG GCC TTG CTC AGC TC-3', reverse: 5'-AGA TTG TGG GCG TCT GTA GG-3'), myosin heavy chain 3 (*Myh3*) forward and reverse primers (forward: 5'-GCC AGG ATG GGA AAG TCA CTG TGG-3', reverse: 5'-GGG CTC GTT CAG GTG GGT CAG C-3'), *Gapdh* forward and reverse primers (forward: 5'-AAC TTT GGC ATT GTG GAA GG-3', reverse: 5'-ACA CAT TGG GGG TAG GAA CA-3'). All qRT-PCR analyses were performed using a Step One Real-Time PCR System (Applied Biosystems). The mRNA levels of *Nos1 μ* , *Pax7*, *MyoD*, *Myogenin*, and *Myh3* were normalized to that of *Gapdh* and quantified using the $\Delta\Delta C_t$ methods. All samples were analyzed in duplicate.

DNA methylation analysis

DNA methylation levels in the *Nos1* promoter region were analyzed using a method described previously [6] (6). Genomic DNA was extracted using the QIAmp DNA Mini Kit (Qiagen, MD, USA). DNA was treated with sodium bisulfite using the Epitect bisulfite kit 48 (Qiagen) according to the manufacturer's instructions. PCR was performed using the TaKaRa EpiTaq HS for bisulfite-treated DNA (Takara Bio, Shiga, Japan) with the *Nos1* forward primer (5'-TTA GTY GGT TGG AYG TTA TTA T-3') and biotinylated reverse primer (5'-CAA CTA CCC CTA ATA AAC AA-3') under the following conditions: an initial denaturation step at 95°C for 3 min, followed by 45 cycles of 95°C for 20 s, 58°C for 20 s, and 72°C for 30 s, and a final extension at 72°C for 5 min. To determine the DNA methylation levels, sequencing was performed with the primer 5'-AAATTTTTTTTAAAGATTTT-TATTGAG-3' using a PyroMark Q96 ID pyrosequencer (Qiagen). Mouse high- and low-methylated genomic DNA (EpigenDX, Hopkinton, MA, USA) were used as positive and negative controls for determining pyrosequencing efficiency. All samples were analyzed in duplicate. In this study, we quantified DNA methylation levels at four sites on the CpG island of the *Nos1* promoter.

Statistical analysis

Data are presented as mean \pm standard error (SE). All the analyses were performed using GraphPad Prism, version 9.0 (GraphPad Software, San Diego, CA, USA). Student's *t*-test was used for all analyses. Nonparametric

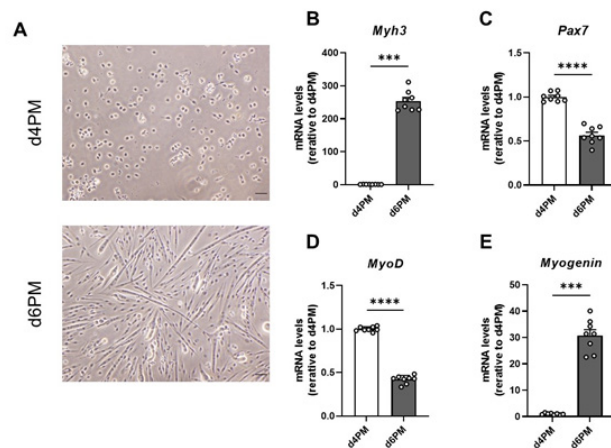


Figure 2. Myogenic marker expression in satellite cell-derived primary myoblast during differentiation. (A) Phase-contrast images of d4PM and d6PM cells. Scale bar = 100 μ m. (B–E) Relative expression levels of *Myh3*, *Pax7*, *MyoD*, and *Myogenin* mRNA in d4PM and d6PM cells. Data represent the means \pm standard error (n=8 per group). *** P < 0.001, **** P < 0.0001; d4PM vs. d6PM. d4PM, day 4 primary myoblasts (undifferentiated); d6PM, day 6 primary myoblasts (differentiated).

data were assessed using the Mann–Whitney *U* test. *P* values <0.05 were considered statistically significant.

Results

Myogenic marker expression in satellite cell-derived primary myoblast during differentiation

The d6PM cells cultured in the differentiation medium for 1 d showed myotube-like shapes compared to the d4PM cells (Figure 2A). The d6PM cells had lower levels of *MyoD* and *Pax7* mRNA and higher levels of *Myogenin* and *Myh3* mRNA compared to the d4PM cells (Figure 2B–E). These data confirmed that d6PM cells are a progressive myogenic differentiation model.

nNOS immunoreactivity was altered and its expression was upregulated in differentiated satellite cell-derived primary myoblasts

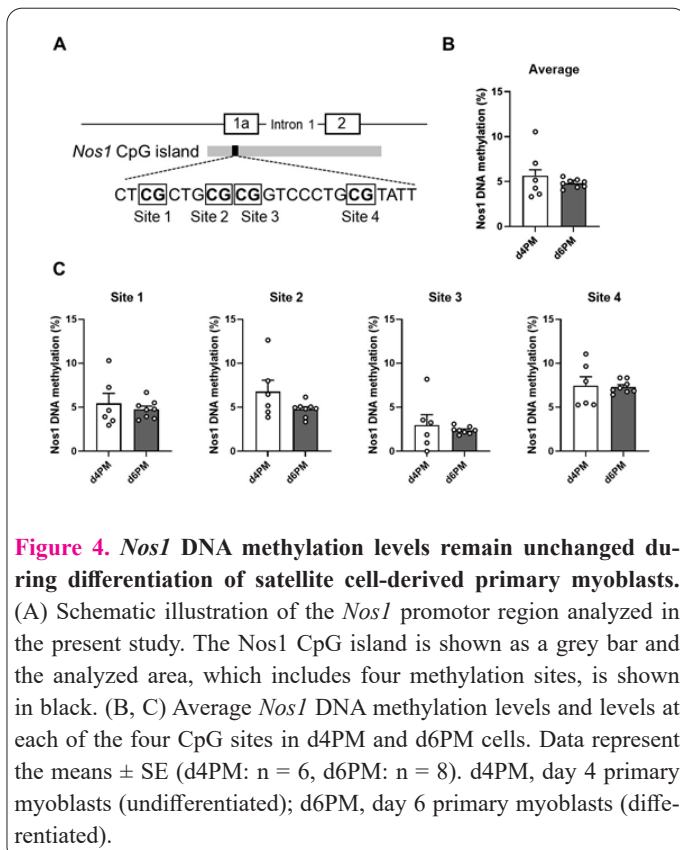
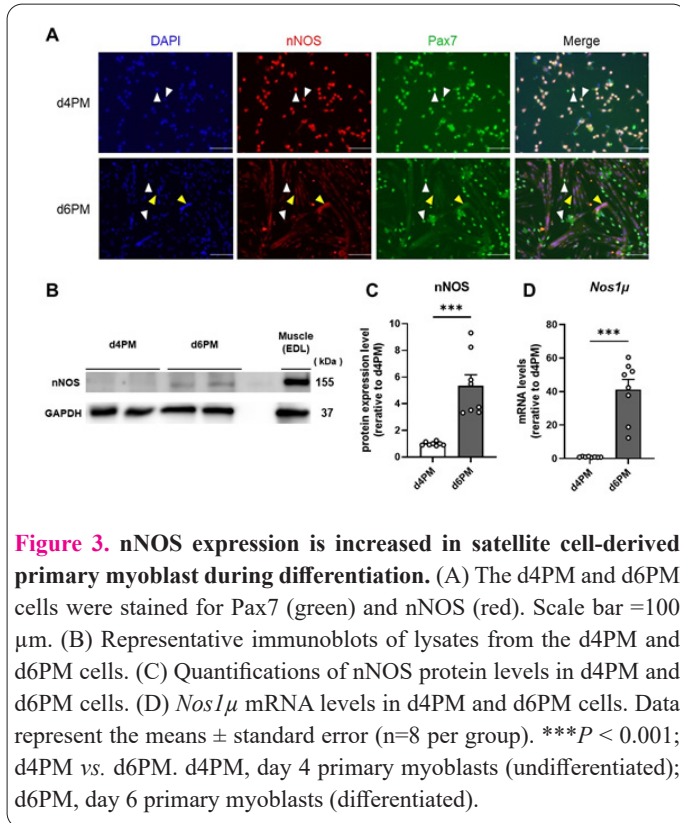
Immunohistochemical analysis showed that d4PM (undifferentiated primary myoblast) cells express Pax7, an activated and quiescent satellite cell marker (Figure 3A). While d6PM cells, the differentiated myotube-like cells did not express Pax7 (Figure 3A). The localization of nNOS in the d4PM and d6PM cells was determined by immunohistochemistry. nNOS immunoreactivity was well-defined in d4PM cells, wherein it colocalized with Pax7 and DAPI (Figure 3A). In contrast, in d6PM cells, nNOS immunoreactivity was spread to the whole myotube-like cells; however, it did not colocalize with DAPI (nucleus marker) or Pax7 (satellite cell marker). The nNOS protein levels, as quantified by western blotting, were higher in d6PM cells compared to those in d4PM cells (Figure 3B, C). These results suggest that satellite cells express nNOS, which translocates from the nucleus to the cytosol and is upregulated during the differentiation process.

Nos1 μ mRNA level was higher in the differentiated d6PM cells compared to that in the differentiated d4PM cells (Figure 3D). Quantitative real-time PCR using exon1-2 specific primer, which can detect both *Nos1 α* and

Nos1 μ isoforms, indicated that while *Nos1 μ* is present in adult skeletal muscles, myoblasts express only *Nos1 α* and myotubes express both *Nos1 α* and *Nos1 μ* (14). These results suggest that mRNA levels of *Nos1*, including *Nos1 α* and *Nos1 μ* , increase in differentiated satellite cell-derived primary myoblasts.

Nos1 DNA methylation levels were unchanged during differentiation

A schematic representation of the four CpG sites loca-



ted in the promoter region of the *Nos1* gene that were analyzed in the present study is shown in Figure 4A. The average *Nos1* DNA methylation levels at the four sites were unchanged in d4PM cells compared to those in the d6PM cells (Figure 4B). Moreover, there were no alterations in the *Nos1* DNA methylation levels at sites 1, 2, 3, and 4 in the d6PM cells compared to that in the d4PM cells (Figure 4C).

Discussion

The key findings of the present study are that, during differentiation, nNOS levels increase in satellite cell-derived primary myoblasts and *Nos1* DNA methylation levels remain unchanged. To investigate the role of nNOS in satellite cells during muscle differentiation, we used a pre-plating method to isolate satellite cells from the gastrocnemius muscle and then cultured them in GM or DM. Immunohistochemical analysis revealed that the levels of the satellite cell marker Pax7 were higher in d4PM cells than in the differentiated myotube-like d6PM cells. The mRNA levels of *Myogenin*, a known differentiation marker, were significantly higher and those of *MyoD* were decreased in differentiated cells than in undifferentiated cells. Satellite cell-derived myoblasts are generally characterized by the same set of myogenic markers as myoblasts derived at almost any developmental stage (15). When satellite cells are activated, they rapidly initiate MyoD expression, followed by myogenin expression, which marks the onset of myogenic differentiation, accompanied by MyoD suppression (15). As Pax7 overexpression downregulates MyoD, prevents myogenin induction, and blocks MyoD-induced myogenic conversion (16), d4PM cells are considered undifferentiated satellite cells. According to Zammit et al. (2006), it is likely that the d6PM cells in this study differentiated from myotubes and matured into myofibers.

We observed nNOS immunoreactivity in Pax7⁺ cells, suggesting that the satellite cells originally expressed nNOS. In mature skeletal muscle, nNOS is located in the nucleus, suggesting that the direct nuclear production of nNOS-derived NO could regulate transcription (17). In the skeletal muscle of old mice, nuclear nNOS protein levels are significantly decreased, whereas nNOS in the cytosolic fraction does not change (18). Thus, nuclear nNOS signaling may contribute to sarcopenia, an age-related loss of skeletal muscle mass.

Previous studies have demonstrated the importance of nuclear nNOS (17, 18). However, as these studies analyzed crude cells, the role of nNOS in satellite cells remains unclear. nNOS immunoreactivity in the nuclei of Pax7⁺ cells was maintained in the differentiated myotube-like cells, followed by the spread of immunoreactivity in the cytosol after differentiation. In addition, nNOS protein and mRNA levels increased during differentiation (Figures 2 and 3). Since nNOS protein levels also increase during differentiation in the C2C12 myoblast cell line (19), differentiation-induced nNOS induction is likely a common event. In adult skeletal muscle, nNOS is largely located in the muscle cell membrane (5). Therefore, as the myogenic lineage progresses, the nNOS localization in satellite cells may change from the nucleus to the cytosol and then cell membrane. Thus, not only quantitative changes in nNOS but also its redistribution in the subcellular fraction of satellite cells during differentiation may contribute to the

regulation of skeletal muscle mass.

DNA methylation is a major epigenetic modification that regulates the differentiation of muscle satellite cells (11). DNMT and TET regulate DNA methylation levels, and demethylation plays an integral role in myogenesis (20-23). We have previously reported that *nNOS* DNA methylation levels are decreased in atrophic muscles (1), suggesting that the epigenetic regulation of *nNOS* is involved in the maintenance of skeletal muscle mass. In the present study, although *nNOS* mRNA levels were significantly increased in differentiated satellite cells, *nNOS* DNA methylation levels were unchanged. Previous studies have reported the methylation sites and tissue-specific-methylation of the *nNOS* DNA promoter region. In adult skeletal muscle, *Nos1* mRNA levels are downregulated in atrophic soleus muscle, accompanied by hypermethylation at sites 1, 2, and 3, but not at site 4 (6). In addition, exercise-induced hypermethylation of the hippocampal *Nos1* promoter differed in the above-mentioned methylation sites and dorsal/ventral regions of the hippocampus (24). Thus, since the *nNOS* promoter region has several methylation sites, other methylation sites may regulate *nNOS* mRNA in myoblasts. Another possible explanation is the presence of several transcription factors. A previous study has reported that some transcription factors regulate *nNOS* mRNA expression levels (25). Further studies are required to determine the mechanism by which *nNOS* mRNA expression in satellite cells is regulated during differentiation.

Taken together, these data suggest that nNOS in satellite cell-derived primary myoblasts may be involved in appropriate muscle differentiation. Although further studies are needed to understand the role of nNOS in various physiological processes involved in the maintenance of skeletal muscle mass, this work provides the basis for understanding the regulation of differentiation in muscle satellite cells.

Acknowledgments

This work was supported in part by the Japan Society for the Promotion of Science (JSPS), KAKENHI (grant numbers 20K20623 and 19H04012 to YH). We thank Ms. Mana Hatanaka for her help with the experiments. We would like to thank Editage (www.editage.com) for English language editing.

Interest conflict

There are no conflicts of interest to declare.

Author's contribution

This work was carried out at Fukuoka University, Fukuoka, Japan. MK, KS, YT, YK and YH conceived and designed the study. MK, KS, AI, and SN performed the experiments. MK, KS and YT analyzed the data. MK, SK, YT, AI, SN, YU, KK, YK and YH interpreted the results. MK and YH prepared the figures. MK, YT, YK and YH drafted the manuscript. All the authors approved the final version of the manuscript submitted for publication.

References

1. Tabara Y, Setoh K, Kawaguchi T, Matsuda F. Skeletal muscle mass index is independently associated with all-cause mortality in men: The Nagahama study. *Geriatr Gerontol Int* 2022; 22(11): 956-960.
2. Li R, Xia J, Zhang XI, Gathirua-Mwangi WG, Guo J, Li Y, McKenzie S, Song Y. Associations of Muscle Mass and Strength with All-Cause Mortality among US Older Adults. *Med Sci Sports Exerc* 2018; 50(3): 458-467.
3. Zammit PS, Golding JP, Nagata Y, Hudon V, Partridge TA, Beauchamp JR. Muscle satellite cells adopt divergent fates: a mechanism for self-renewal? *J Cell Biol* 2004; 166(3): 347-57.
4. Kitajima Y, Suzuki N, Nunomiya A, Osana S, Yoshioka K, Tashiro Y, Takahashi R, Ono Y, Aoki M, Nagatomi R. The Ubiquitin-Proteasome System Is Indispensable for the Maintenance of Muscle Stem Cells. *Stem Cell Rep* 2018; 11(6): 1523-1538.
5. Kobzik L, Reid MB, Bredt DS, Stamler JS. Nitric oxide in skeletal muscle. *Nature* 1994; 372(6506): 546-8.
6. Tomiga Y, Ito A, Sudo M, Ando S, Eshima H, Sakai K, Nakashima S, Uehara Y, Tanaka H, Soejima H, Higaki Y. One week, but not 12 hours, of cast immobilization alters promoter DNA methylation patterns in the nNOS gene in mouse skeletal muscle. *J Physiol* 2019; 597(21): 5145-5159.
7. Suzuki N, Motohashi N, Uezumi A, Fukada S, Yoshimura T, Itoyama Y, Aoki M, Miyagoe-Suzuki Y, Takeda S. NO production results in suspension-induced muscle atrophy through dislocation of neuronal NOS. *J Clin Invest* 2007; 117(9): 2468-76.
8. Ito N, Ruegg UT, Kudo A, Miyagoe-Suzuki Y, Takeda S. Activation of calcium signaling through Trpv1 by nNOS and peroxynitrite as a key trigger of skeletal muscle hypertrophy. *Nat Med* 2013; 19(1): 101-6.
9. Buono R, Vantaggiato C, Pisa V, Azzoni E, Bassi MT, Brunelli S, Sciorati C, Clementi E. Nitric oxide sustains long-term skeletal muscle regeneration by regulating fate of satellite cells via signaling pathways requiring Vangl2 and cyclic GMP. *Stem Cells* 2012; 30(2): 197-209.
10. Church JE, Gehrig SM, Chee A, Naim T, Trieu J, McConell GK, Lynch GS. Early functional muscle regeneration after myotoxic injury in mice is unaffected by nNOS absence. *Am J Physiol Regul Integr Comp Physiol* 2011; 301(5): R1358-66.
11. Hatazawa Y, Ono Y, Hirose Y, Kanai S, Fujii NL, Machida S, Nishino I, Shimizu T, Okano M, Kamei Y, Ogawa Y. Reduced Dnmt3a increases Gdf5 expression with suppressed satellite cell differentiation and impaired skeletal muscle regeneration. *FASEB J* 2018; 32(3): 1452-1467.
12. K. Yoshioka, Y. Kitajima, N. Okazaki, K. Chiba, A. Yonekura, Y. Ono, A modified pre-plating method for high-yield and high-purity muscle stem cell isolation from human/mouse Skeletal Muscle tissues, *Front Cell Dev Biol* 8 (2020) 1–7.
13. Kitajima Y, Ono Y. Visualization of PAX7 protein dynamics in muscle satellite cells in a YFP knock-in-mouse line. *Skeletal Muscle* 2018; 8(1): 26.
14. Silvagno F, Xia H, Bredt DS. Neuronal nitric-oxide synthase-mu, an alternatively spliced isoform expressed in differentiated skeletal muscle. *J Biol Chem* 1996; 271(19): 11204-8.
15. Zammit PS, Partridge TA, Yablonka-Reuveni Z. The skeletal muscle satellite cell: the stem cell that came in from the cold. *J Histochem Cytochem* 2006; 54(11): 1177-91.
16. Olguin HC, Olwin BB. Pax-7 up-regulation inhibits myogenesis and cell cycle progression in satellite cells: a potential mechanism for self-renewal. *Dev Biol* 2004; 275(2): 375-88.
17. Aquilano K, Baldelli S, Ciriolo MR. Nuclear recruitment of neuronal nitric-oxide synthase by α -syn-trophin is crucial for the induction of mitochondrial biogenesis. *J Biol Chem* 2014; 289(1): 365-78.
18. Baldelli S, Ciriolo MR. Altered S-nitrosylation of p53 is responsible for impaired antioxidant response in skeletal muscle during aging. *Aging (Albany NY)* 2016; 8(12): 3450-3467.
19. Montagna C, Rizza S, Ciriotti C, Maiani E, Muscaritoli M, Musarò

- A, Carrí MT, Ferraro E, Cecconi F, Filomeni G. nNOS/GSNOR interaction contributes to skeletal muscle differentiation and homeostasis. *Cell Death Dis* 2019; 10(5): 354.
20. Fong AP, Yao Z, Zhong JW, Cao Y, Ruzzo WL, Gentleman RC, Tapscott SJ. Genetic and epigenetic determinants of neurogenesis and myogenesis. *Dev Cell* 2012; 22(4): 721-35.
21. Laker RC, Ryall JG. DNA Methylation in Skeletal Muscle Stem Cell Specification, Proliferation, and Differentiation. *Stem Cells Int* 2016; 2016: 5725927.
22. Liu R, Kim KY, Jung YW, Park IH. Dnmt1 regulates the myogenic lineage specification of muscle stem cells. *Sci Rep* 2016; 6: 35355.
23. Rugowska A, Starosta A, Konieczny P. Epigenetic modifications in muscle regeneration and progression of Duchenne muscular dystrophy. *Clin Epigenetics* 2021; 13(1): 13.
24. Tomiga Y, Sakai K, Ra SG, Kusano M, Ito A, Uehara Y, Takahashi H, Kawanaka K, Soejima H, Higaki Y. Short-term running exercise alters DNA methylation patterns in neuronal nitric oxide synthase and brain-derived neurotrophic factor genes in the mouse hippocampus and reduces anxiety-like behaviors. *FASEB J* 2021; 35(8): e21767.
25. Saur D, Seidler B, Paehge H, Schusdziarra V, Allescher HD. Complex regulation of human neuronal nitric-oxide synthase exon 1c gene transcription. Essential role of Sp and ZNF family members of transcription factors. *J Biol Chem* 2002; 277(28): 25798-814